

# Magnetic phase transitions and ferromagnetic short-range correlations in single-crystal $\text{Tb}_5\text{Si}_{2.2}\text{Ge}_{1.8}$

M. Zou, V. K. Pecharsky,\* and K. A. Gschneidner, Jr.

Ames Laboratory of the U.S. DOE, Iowa State University, Ames, Iowa 50011-3020, USA  
and Department of Materials Science and Engineering, Iowa State University, Ames, Iowa 50011-2300, USA

D. L. Schlager and T. A. Lograsso

Ames Laboratory of the U.S. DOE, Iowa State University, Ames, Iowa 50011-3020, USA

(Received 24 April 2008; published 31 July 2008)

Magnetic phase transitions in a  $\text{Tb}_5\text{Si}_{2.2}\text{Ge}_{1.8}$  single crystal have been studied as a function of temperature and magnetic field. Magnetic-field dependencies of the critical temperatures are highly anisotropic for both the main magnetic ordering process occurring around 120 K and a spin reorientation transition at  $\sim 70$  K. Magnetic-field-induced phase transitions occur with the magnetic field applied isothermally along the  $a$  and  $b$  axes (but not along the  $c$  axis) between 1.8 and 70 K in fields below 70 kOe. Strong anisotropic thermal irreversibility is observed in the Griffiths phase regime between 120 and 200 K with applied fields ranging from 10 to 1000 Oe. Our data (1) show that the magnetic and structural phase transitions around 120 K are narrowly decoupled; (2) uncover the anisotropy of ferromagnetic short-range order in the Griffiths phase; and (3) reveal some unusual magnetic domain effects in the long-range ordered state of the  $\text{Tb}_5\text{Si}_{2.2}\text{Ge}_{1.8}$  compound. The temperature-magnetic field phase diagrams with field applied along the three major crystallographic directions have been constructed.

DOI: 10.1103/PhysRevB.78.014435

PACS number(s): 75.30.Kz, 75.30.Gw, 75.40.-s, 75.50.Cc

## I. INTRODUCTION

The  $R_5(\text{Si}_x\text{Ge}_{1-x})_4$  intermetallic compounds, where  $R$  is a rare-earth element, were brought to the forefront of materials physics after the discovery of the giant magnetocaloric effect in  $\text{Gd}_5(\text{Si}_{0.5}\text{Ge}_{0.5})_4$ .<sup>1</sup> Other interesting phenomena, including the colossal magnetostriction,<sup>2</sup> giant magnetoresistance,<sup>3</sup> and spontaneous generation of voltage<sup>4</sup> were observed in these alloys soon after. The unusually strong magneto-responsiveness in the  $\text{Gd}_5(\text{Si}_x\text{Ge}_{1-x})_4$  systems is due to first-order magnetic martensitic-like transitions which can be triggered reversibly by temperature, magnetic field, and pressure.<sup>5</sup>

The  $\text{Tb}_5(\text{Si}_x\text{Ge}_{1-x})_4$  system is the second most studied subset in the family of  $R_5(\text{Si}_x\text{Ge}_{1-x})_4$  alloys. The Tb-based compounds exhibit the giant magnetocaloric effect in the intermediate range of compositions,  $0.35 < x < 0.65$ .<sup>6-9</sup> The crystallographic transformation in  $\text{Tb}_5(\text{Si}_x\text{Ge}_{1-x})_4$  between the monoclinic and orthorhombic polymorphs, and the magnetic ordering-disordering phase transition between the paramagnetic and canted ferromagnetic states (henceforth referred to as simply “ferromagnetic,” also see Fig. 1), which are different from  $\text{Gd}_5(\text{Si}_x\text{Ge}_{1-x})_4$ , are decoupled by about 10 K and less than 5 K when  $x=0.5$  and  $0.55$ , respectively.<sup>10,11</sup> Moreover, the separate crystallographic and magnetic phase transitions can be recoupled in a polycrystalline  $\text{Tb}_5\text{Si}_2\text{Ge}_2$  by applying hydrostatic pressures greater than 8.6 kbar,<sup>12</sup> or by magnetic fields greater than 10 kOe when applied along the easy magnetization direction, i.e., along the  $a$  axis, of a  $\text{Tb}_5\text{Si}_{2.2}\text{Ge}_{1.8}$  single crystal.<sup>13</sup> In either case, the compound transforms from the monoclinic paramagnetic to the orthorhombic ferromagnetic state. External magnetic fields up to 70 kOe applied along the magnetically hard direction, i.e., along the  $b$  axis of single crystalline  $\text{Tb}_5\text{Si}_{2.2}\text{Ge}_{1.8}$ , are not

strong enough to induce the paramagnetic to ferromagnetic phase transition at temperatures slightly higher than the zero field  $T_C$ .<sup>13</sup> However, fields between 60 and 70 kOe can trigger the paramagnetic to ferromagnetic transition when applied along the  $c$  axis.<sup>13</sup>

Although a study of the field-induced magnetostructural transition of  $\text{Tb}_5\text{Si}_{2.2}\text{Ge}_{1.8}$  has been reported,<sup>13</sup> experimental data about the temperature-dependent behavior in different magnetic fields are lacking. Knowing the latter, however, is important because the decoupling of the magnetic and struc-

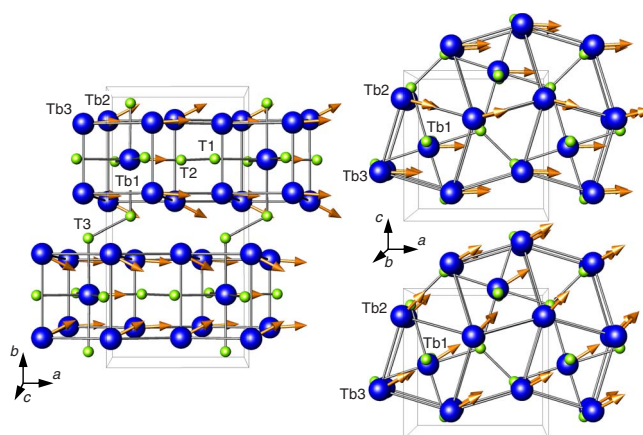


FIG. 1. (Color online) Crystal and magnetic structures of  $\text{Tb}_5\text{Si}_{2.2}\text{Ge}_{1.8}$  following Ref. 11. The left panel shows the magnetic structure between 75 and  $\sim 120$  K and it also highlights the connectivity of the slabs via  $-\text{Tb}1-\text{T}3-\text{T}3-\text{Tb}1-$  bonds. The top panel on the right shows the orientations of the magnetic moments of the Tb atoms in one slab between 75 and  $\sim 120$  K. The bottom panel on the right shows the orientations of the magnetic moments in one slab below 75 K. T1, T2, and T3 represent a statistical mixture of Si and Ge atoms of the 2.2:1.8 (0.55:0.45) atomic ratio.

tural phase transitions in  $\text{Tb}_5(\text{Si}_x\text{Ge}_{1-x})_4$  leads to a complicated crystallographic and magnetic phase coexistence near  $T_C$ . Furthermore, intrinsic twinning at the nanoscale<sup>14</sup> in the monoclinic phase enhances the Griffiths-like phase behavior in polycrystalline  $\text{Tb}_5\text{Si}_2\text{Ge}_2$ , which is detected by the less-than-unity exponent of the inverse susceptibility in magnetic fields between 1 and 1500 Oe due to ferromagnetic short-range order.<sup>15</sup> Anisotropic ferromagnetic short-range order has been observed in both antiferromagnetic and paramagnetic states of single crystal  $\text{Gd}_5\text{Ge}_4$ , and was ascribed to the anisotropy of the layered crystal structure of the  $\text{Gd}_5\text{Ge}_4$  compound considering negligible single-ion anisotropy of  $\text{Gd}^{3+}$ .<sup>16</sup> The anisotropy is expected to be much enhanced when  $R=\text{Tb}$ .

Another substantial difference between the magnetic properties of  $\text{Tb}_5(\text{Si}_x\text{Ge}_{1-x})_4$  and  $\text{Gd}_5(\text{Si}_x\text{Ge}_{1-x})_4$  in the intermediate range of compositions is the presence of spin reorientation transitions, which occur in  $\text{Tb}_5(\text{Si}_x\text{Ge}_{1-x})_4$  at  $T_{\text{SR}} \cong 70$  K and 75 K when  $x=0.5$  and 0.55, respectively, well below their magnetic order-disorder transformations at  $\sim 120$  K. The spin reorientation transitions separating two different ferromagnetic states in  $\text{Tb}_5(\text{Si}_x\text{Ge}_{1-x})_4$ ,<sup>9,11</sup> are absent in  $\text{Gd}_5(\text{Si}_x\text{Ge}_{1-x})_4$ . Below and above  $T_{\text{SR}}$ , the magnetic structure remains canted ferromagnetically along the  $a$  axis, but the moments tilt further away from the  $a$  axis upon cooling as can be seen in Fig. 1. The antiferromagnetically aligned moment components along the  $b$  axis vary insignificantly both in their directions and magnitudes during this spin reorientation transition. The  $c$ -axis components, however, change from antiferromagnetic above  $T_{\text{SR}}$  to a ferromagnetic alignment below  $T_{\text{SR}}$ . There is no apparent crystallographic change associated with these spin reorientation transitions in either  $\text{Tb}_5\text{Si}_2\text{Ge}_2$  or  $\text{Tb}_5\text{Si}_{2.2}\text{Ge}_{1.8}$ . According to the neutron-diffraction study of  $\text{Tb}_5\text{Si}_{2.2}\text{Ge}_{1.8}$ ,<sup>11</sup> the spontaneous magnetic moments of Tb atoms located in three inequivalent crystallographic sites have different canting angles, indicating different local magnetocrystalline anisotropy of Tb moments.

To carry out a systematic study of the magnetization of  $\text{Tb}_5\text{Si}_{2.2}\text{Ge}_{1.8}$  compound and to further explore the anisotropy of the Griffiths phase behavior, the temperature and magnetic-field dependencies of the dc magnetization along the three principal crystallographic axes of a high-purity  $\text{Tb}_5\text{Si}_{2.2}\text{Ge}_{1.8}$  single crystal are presented. Our results show a complicated magnetic behavior as a function of temperature, magnetic-field, and crystallographic directions. A strong anisotropy was observed in the Griffiths phase regime, and is likely responsible for the low-field (less than 1000 Oe) thermal history dependencies of the magnetization of the compound.

## II. EXPERIMENTAL DETAILS

$\text{Tb}_5\text{Si}_{2.2}\text{Ge}_{1.8}$  single crystal for the magnetization measurements was grown by the tri-arc method<sup>17</sup> from high-purity Tb, Si, and Ge mixed in appropriate quantities. The Tb was prepared by the Materials Preparation Center<sup>18</sup> and contained the following major impurities (in ppm at.): O, 1900; C, 1100; N, 180; F, 40; Cl, 33; thus it was approximately

99.67 at. % (99.97 wt %) pure. The Si and Ge were purchased from Meldform Metals Ltd. and were better than 99.999 wt % pure. The as-grown crystal was oriented by using backscattered Laue x-ray diffraction. A sample for the magnetization measurements was cut by spark erosion. The sample was in the form of a parallelepiped with dimensions of  $1.50 \times 1.94 \times 0.88$  mm<sup>3</sup> along the  $a$ ,  $b$ , and  $c$ -axes directions, respectively, and weighed 18.73 mg.

The temperature ( $T$ ) and magnetic-field ( $H$ ) dependencies of the magnetization ( $M$ ) were measured from 1.8 to 300 K in constant magnetic fields of 0.01, 0.1, 1, 10, and 50 kOe, and from 0 to 70 kOe at various constant temperatures ranging between 1.8 and 70 K in a superconducting quantum interference device (SQUID) magnetometer, MPMS-XL from Quantum Design, Inc. When measuring  $M(T)$ , three sets of data were collected for every fixed applied magnetic field and orientation of the single crystal. The first one was collected upon heating in a constant magnetic field applied at the lowest temperature after the sample was zero field cooled (ZFC) from a temperature well above its Curie temperature ( $T_C$ ). The second and third ones were collected upon cooling and heating in the same field strength as that in the first, ZFC heating measurement. The first set of data is referred to as ZFC heating, the second as field-heated (FH) cooling, and the third one as field-cooled (FC) heating hereafter. Every isothermal  $M(H)$  measurement was recorded after thermal demagnetization at 250 K and then zero field cooling down to the measurement temperature. The applied magnetic fields varied from 0 to 70 kOe with a 2 kOe step. The misalignment between the directions of the magnetic-field vector and the crystal axes was less than  $\pm 5^\circ$ , considering the combined accuracy of crystallographic alignment and sample positioning inside the cryostat.

## III. RESULTS AND DISCUSSION

Temperature dependencies of the magnetization of single-crystal  $\text{Tb}_5\text{Si}_{2.2}\text{Ge}_{1.8}$  measured in a 10 kOe magnetic field applied along the  $a$ ,  $b$ , and  $c$ -axes directions between 1.8 and 200 K are shown in Fig. 2. The FC heating and FH cooling data overlap over the entire temperature range except for small differences at  $T_C$ , i.e., hystereses along the  $a$  and  $c$  axes, and a spike along the  $b$  axis. Thus, only ZFC heating and FH cooling data are displayed for clarity.

The  $M(T)$  behaviors shown in Fig. 2 exhibit several noteworthy features. First, below  $T_C \cong 120$  K, the magnitudes of the magnetization with  $\mathbf{H} \parallel \mathbf{a}$  and  $\mathbf{H} \parallel \mathbf{c}$  are much greater than those with  $\mathbf{H} \parallel \mathbf{b}$ . This is in line with the magnetic structure of this compound,<sup>11</sup> where the magnetic moments are mainly confined to the  $ac$  plane (see Fig. 1). Second, a cusp in the  $\mathbf{H} \parallel \mathbf{a}$  and  $\mathbf{H} \parallel \mathbf{b}$   $M(T)$  curves, and a minimum in the first derivative of magnetization with respect to temperature ( $dM/dT$ ) with  $\mathbf{H} \parallel \mathbf{c}$  (inset of Fig. 2) are consistent with a spin reorientation transition at  $\sim 70$  K. With  $\mathbf{H} \parallel \mathbf{a}$ , the magnetization increasing on heating from 2 to 70 K is in agreement with decreasing of the average angle that the Tb moments form with the  $a$  axis from  $38.4^\circ$  at 4.2 K to  $9.3^\circ$  at 75 K.<sup>11</sup> From 70 to about 120 K magnetization with  $\mathbf{H} \parallel \mathbf{a}$  shows a typical ferromagnetic behavior as the magnetic structure

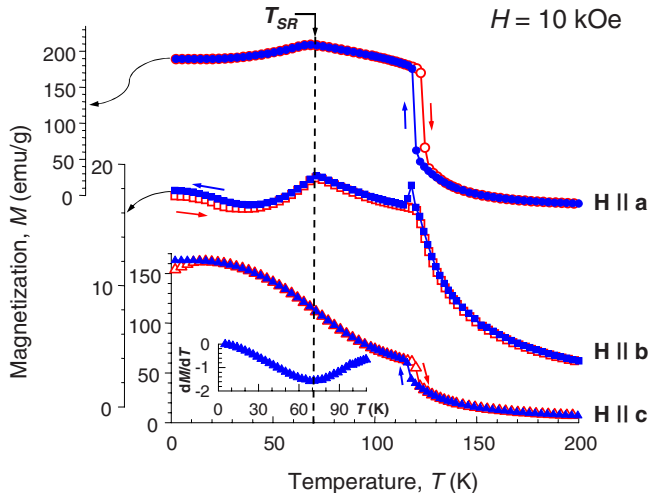


FIG. 2. (Color online) Temperature dependencies of the magnetization of single-crystal  $\text{Tb}_5\text{Si}_{2.2}\text{Ge}_{1.8}$  measured in a 10 kOe magnetic field applied parallel to the  $a$ ,  $b$ , and  $c$  axes upon ZFC heating (open symbols) and FH cooling (solid symbols). The inset is the temperature dependence of the first derivative of the magnetization with respect to temperature ( $dM/dT$ ) when  $\mathbf{H}\parallel c$  upon FH cooling. Note that the temperature scale is the same for the three orientations.

along the  $a$  axis remains unchanged. The magnetic-moment component along the  $c$  axis switches from a ferromagnetic to an antiferromagnetic configuration upon heating through 70 K.<sup>11</sup> This corresponds to a change of the sign of  $dM/dT$  when the magnetic field is parallel to the spin axis, i.e., the ferromagnetic susceptibility decreases, while an antiferromagnetic susceptibility increases upon heating. Consequently, a  $dM/dT$  minimum is formed at 70 K with  $\mathbf{H}\parallel c$ .

When  $\mathbf{H}\parallel b$ , the magnetization values initially decrease with increasing temperature from 1.8 K, form a minimum at about 40 K, and then reach a maximum at 70 K. Contrary to  $\mathbf{H}\parallel a$  and  $\mathbf{H}\parallel c$ , this behavior does not follow the thermal evolution of the  $b$ -axis components of spontaneous magnetic moments in zero field.<sup>11</sup> Recalling that measured magnetization also manifests the ability of the external field to overcome the magnetocrystalline anisotropy energy, magneto-static energy, and thermal fluctuations to align the moments in the field direction, the complicated thermal variation of the magnetization with  $\mathbf{H}\parallel b$  may reflect the thermal dependence of the magnetic anisotropy energy. When  $70\text{ K} < T < \sim 120\text{ K}$ , the magnetization with  $\mathbf{H}\parallel b$  continuously decreases upon heating. Upon FH cooling, however, a sharp spike develops at 118 K. The explanation of the physical origin of this singularity will be given below during the discussion of the low-field temperature dependencies of the magnetization of  $\text{Tb}_5\text{Si}_{2.2}\text{Ge}_{1.8}$ .

The magnetic order-disorder transition, which occurs around 120 K, shows a thermal hysteresis of 4 K when  $\mathbf{H}\parallel a$  and  $\mathbf{H}\parallel c$ , which signifies a first-order phase transition, but the hysteretic behavior is different when  $\mathbf{H}\parallel b$ . In the  $R_5(\text{Si}_x\text{Ge}_{1-x})_4$  family with  $R=\text{Gd}$ , the first-order magnetic order-disorder transition is always a coupled magnetic and crystallographic phase transition.<sup>5</sup> For example, in  $\text{Gd}_5\text{Si}_2\text{Ge}_2$  compound, which is analogous to  $\text{Tb}_5\text{Si}_{2.2}\text{Ge}_{1.8}$ ,

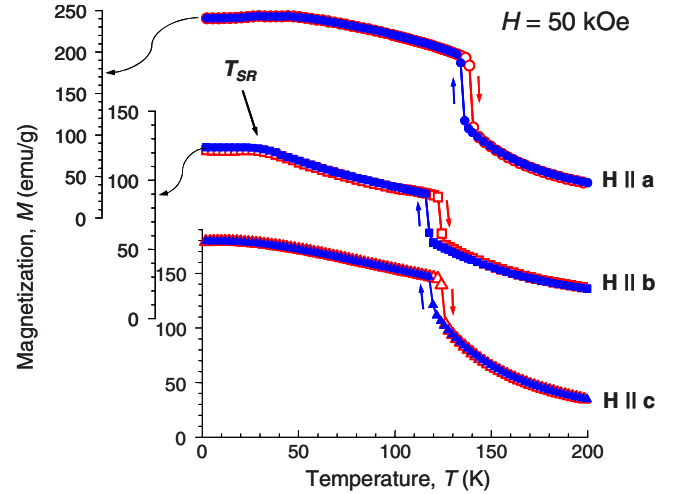


FIG. 3. (Color online) Temperature dependencies of the magnetization of single-crystal  $\text{Tb}_5\text{Si}_{2.2}\text{Ge}_{1.8}$  measured in a 50 kOe magnetic field applied parallel to the  $a$ ,  $b$ , and  $c$  axes upon ZFC heating (open symbols) and FH cooling (solid symbols). Note that the temperature scale is the same for all three orientations.

the transformation from a high-temperature monoclinic to a low-temperature orthorhombic phase is simultaneously accompanied by a paramagnetic to ferromagnetic transition. In  $\text{Tb}_5(\text{Si}_x\text{Ge}_{1-x})_4$ , however, these two transitions (magnetic and crystallographic) may be decoupled, and the extent of decoupling is composition dependent.<sup>10-13</sup> Since decoupling in  $\text{Tb}_5\text{Si}_{2.2}\text{Ge}_{1.8}$  is less than 5 K, and the two transitions can be recoupled by applying  $H \geq 10$  kOe when  $\mathbf{H}\parallel a$ ,<sup>13</sup> the magnetic order-disorder transitions shown in Fig. 2 with  $\mathbf{H}\parallel a$  and  $\mathbf{H}\parallel c$  are likely coupled magnetostructural phase transformations. The difference in hysteretic behavior when  $\mathbf{H}\parallel b$  is due to the fact that the 10 kOe magnetic field is not strong enough to align the moments in the field direction. This explanation is consistent with temperature dependencies of the magnetization measured in a 50 kOe applied magnetic field, which are shown in Fig. 3. Only ZFC heating and FH cooling results are displayed here because the ZFC and FC heating data are identical.

From Fig. 3, one can see that the magnetic order-disorder transitions exhibit very similar thermal hystereses regardless of the direction of the 50 kOe magnetic field. The magnitudes of the magnetization at temperatures immediately below the ferromagnetic to paramagnetic transition are equivalent to  $6.7\mu_B$ ,  $3.1\mu_B$ , and  $5.1\mu_B$  per Tb atom with  $\mathbf{H}\parallel a$ ,  $\mathbf{H}\parallel b$ , and  $\mathbf{H}\parallel c$ , respectively. Taking the value with  $\mathbf{H}\parallel a$  as a reference, the relative collinearity of the magnetic moments with applied magnetic field is 100%, 47%, and 76% with  $\mathbf{H}\parallel a$ ,  $\mathbf{H}\parallel b$ , and  $\mathbf{H}\parallel c$ , respectively. Similarity of hysteretic behaviors shown in Fig. 3 with those observed in numerous  $\text{Gd}_5(\text{Si}_x\text{Ge}_{1-x})_4$  compounds indicates that when a sufficient fraction of magnetic moments is aligned with the external field, the magnetic order-disorder transition in  $\text{Tb}_5\text{Si}_{2.2}\text{Ge}_{1.8}$  becomes first-order and is likely a coupled magnetic and crystallographic phase transition. The transition takes place at different temperatures when the 50 kOe magnetic field is applied along different directions. Consistent with the relative collinearity of the moments, the transition temperature is



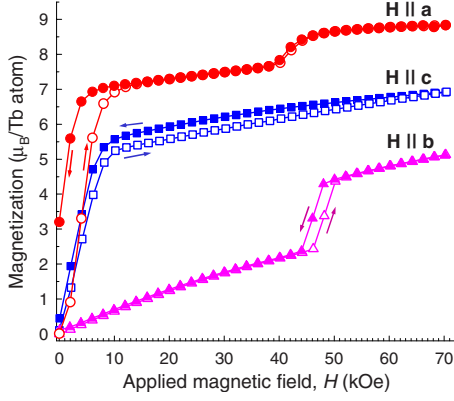


FIG. 4. (Color online) Magnetization isotherms of single-crystal  $\text{Tb}_5\text{Si}_{2.2}\text{Ge}_{1.8}$  measured with the applied magnetic field parallel to the  $a$ ,  $b$ , and  $c$  axes at 1.8 K. The open symbols are field increasing and the solid symbols are field decreasing data points.

the highest with  $\mathbf{H}\parallel\mathbf{a}$ , the lowest with  $\mathbf{H}\parallel\mathbf{b}$ , and it is intermediate with  $\mathbf{H}\parallel\mathbf{c}$ . This is expected because states with greater disorder ( $\mathbf{H}\parallel\mathbf{b}$  and  $\mathbf{H}\parallel\mathbf{c}$ ) can be destroyed by lower thermal energy. Moreover, wider hystereses are associated with lower magnetic ordering temperatures when  $\mathbf{H}\parallel\mathbf{b}$  ( $\sim 6$  K) and  $\mathbf{H}\parallel\mathbf{c}$  ( $\sim 5$  K) compared to  $\sim 4$  K when  $\mathbf{H}\parallel\mathbf{a}$ . The hysteresis generally arises from the need to overcome some energy barriers separating neighboring low energy states, which in this case, is mainly strain due to the crystallographic phase transformation. As the transition temperature lowers, the widening hysteresis reflects complexity of the energy landscape in  $\text{Tb}_5\text{Si}_{2.2}\text{Ge}_{1.8}$ .

Figure 3 also shows that the spin reorientation transition either shifts to lower temperature in a 50 kOe magnetic field ( $\mathbf{H}\parallel\mathbf{b}$ ) or becomes indistinguishable ( $\mathbf{H}\parallel\mathbf{a}$  and  $\mathbf{H}\parallel\mathbf{c}$ ) when compared to the 10 kOe data of Fig. 2. This is expected because at  $T_{\text{SR}}$ , the orientations of Tb moments change within the  $ac$  plane, and applying higher magnetic field within the same plane is more effective in aligning the moments. Consequently,  $T_{\text{SR}}$  becomes indistinguishable when the moments remain mostly aligned with the 50 kOe field regardless of temperature as long as it remains below  $T_C$ .

The significant difference between the temperature dependence of the magnetization with 10 and 50 kOe external fields applied parallel to the three principal crystallographic axes indicates a complicated thermal evolution of the magnetic structure of  $\text{Tb}_5\text{Si}_{2.2}\text{Ge}_{1.8}$  in the presence of external magnetic fields. This may be further probed by measuring magnetization isotherms at different temperatures with magnetic field applied along the three major crystal axes.

Figure 4 shows the magnetization isotherms of the  $\text{Tb}_5\text{Si}_{2.2}\text{Ge}_{1.8}$  single crystal measured at 1.8 K. The magnetization with  $\mathbf{H}\parallel\mathbf{a}$  involves a two-step process. The first step corresponds to the domain-wall movement when the applied field is increased from 0 to 6 kOe and it then continues as a slow increase of the magnetization due to a coherent rotation of magnetic moments toward the direction of the applied field from 8 to 38 kOe. Two facts are noted: (i) no hysteresis occurs when the applied field is greater than 10 kOe, and (ii) the magnetization at  $H=10$  kOe is  $7.4\mu_B$  per Tb atom, which is close to the value of the average  $a$  axis component

( $7.3\mu_B$  per Tb atom) obtained from the neutron-diffraction study. Hence, from 10 to 38 kOe, the material is a single domain with a major ferromagnetic component of all magnetic moments along the  $a$  axis (see Fig. 1). Note, that at this point the magnetic moments in the domain have substantial canting angles with the  $a$  axis. The second step of magnetization starts with a rapid increase when the applied field is between 40 and 48 kOe, indicating that the magnetic structure of  $\text{Tb}_5\text{Si}_{2.2}\text{Ge}_{1.8}$  has changed. This step brings a nearly full alignment of moments along the external field direction because the magnetization value at  $H=48$  kOe is  $9.3\mu_B$  per Tb atom, close to the  $9.4\mu_B$  per Tb atom obtained from the neutron-diffraction measurements at 4.2 K, and to the theoretically expected value of  $gJ=9\mu_B$ . The excess of  $0.3\mu_B$  reflects contribution from itinerant  $5d$  electrons of Tb. There is only a narrow hysteresis associated with this magnetic phase transition.

Since the magnetic moments are mainly confined to the  $ac$  plane of the  $\text{Tb}_5\text{Si}_{2.2}\text{Ge}_{1.8}$  crystal lattice, the nearly linear increase of the magnetization upon increasing the applied field from 0 to 46 kOe in the  $b$ -axis direction is due to a continuous rotation of the magnetic moments toward the external field direction. This rotation is reversible, and consequently, there is no hysteresis. A discontinuous increase by  $1.9\mu_B$  per Tb atom occurs between 46 and 50 kOe. This discontinuity indicates a sudden change of the orientation of some of the magnetic moments when the external field overcomes the anisotropy energy. We argue that this field-induced magnetic phase transition is a result of flipping the moments at the Tb1 sites (see Fig. 1) out of the  $ac$  plane and becoming parallel to the  $b$  axis. Recall that the Tb1 moments are perpendicular to the  $b$  axis in a zero magnetic field. Of the Tb sites in the  $\text{Sm}_5\text{Ge}_4$ -type structure, 20% are Tb1 sites and the remaining 80% are equally divided between Tb2 and Tb3. Thus, flipping all Tb1 moments from perpendicular to parallel to the external field, should suddenly increase magnetization by  $\sim 20\%$  of the full magnetic moment of the Tb atom ( $9.3\mu_B \times 20\% = 1.9\mu_B$ ). A hysteresis of about 2 kOe accompanies this transition, which also indicates a strong magnetoelastic effect.

Although the magnetic moments are mainly confined to the  $ac$  plane, the magnetization at 1.8 K with  $\mathbf{H}\parallel\mathbf{c}$  shows quite different features from that with  $\mathbf{H}\parallel\mathbf{a}$ . First, there is a hysteresis between the field increasing and decreasing branches over the entire range of fields, suggesting that besides being dominant during the initial magnetization process between 0 and 6 kOe, the domain-wall movements accompany the coherent magnetic-moment rotation between 8 and 70 kOe. Second, the magnitude of the magnetization at  $H=10$  kOe, equivalent to  $5.2\mu_B/\text{Tb}^{3+}$ , is only slightly smaller than  $5.5\mu_B$ —the  $c$ -axis component of the spontaneous magnetization at 4.2 K. These two observations mean that the material is close to but not completely in a single domain state when the applied field is greater than 10 kOe and applied in the  $c$ -axis direction. Therefore, domain walls are not as mobile when  $\mathbf{H}\parallel\mathbf{c}$  when compared to  $\mathbf{H}\parallel\mathbf{a}$ . Consequently, a smaller remanent magnetization mainly due to domain-wall pinning is observed with  $\mathbf{H}\parallel\mathbf{c}$  than with  $\mathbf{H}\parallel\mathbf{a}$ . Third, the absence of magnetization jump(s), such as those observed with  $\mathbf{H}\parallel\mathbf{a}$  between 40 and 48 kOe, and with  $\mathbf{H}\parallel\mathbf{b}$  between 46

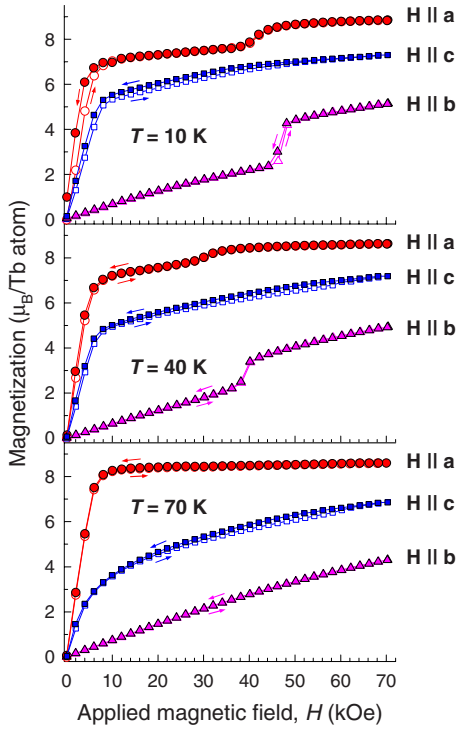


FIG. 5. (Color online) Magnetization isotherms of single-crystal  $\text{Tb}_5\text{Si}_{2.2}\text{Ge}_{1.8}$  measured with the applied magnetic field parallel to the  $a$ ,  $b$ , and  $c$  axes and varying from 0 to 70 kOe at 10, 40, and 70 K. The open symbols are field increasing and the solid symbols are field decreasing data points.

and 50 kOe, indicates that there is no field-induced magnetic phase transition below 70 kOe with  $\mathbf{H}\parallel\mathbf{c}$ . This is in line with the neutron-diffraction observation<sup>11</sup> that the Tb moment projection along the  $c$  axis is ferromagnetic at low temperature.

The magnetic phase transitions that occur at 1.8 K when the magnetic field is applied along the  $a$ - and  $b$ -axes directions result from a competition between the magnetocrystalline anisotropy and the external field. Since the magnetocrystalline anisotropy generally varies with temperature, it is reasonable to expect such transitions to occur at different critical magnetic fields as temperature varies. When the system reaches the spin reorientation temperature,  $T_{\text{SR}}=70$  K, the magnetic moments are almost collinear in the  $a$ -axis direction, therefore, the magnetic field applied in this direction needed to induce the magnetic phase transition isothermally should be lower. This is indeed the case when the magnetization of the  $\text{Tb}_5\text{Si}_{2.2}\text{Ge}_{1.8}$  single crystal was measured isothermally as a function of applied magnetic field between 1.8 and 70 K; representative isotherms at 10, 40, and 70 K are shown in Fig. 5. The values of the critical fields decrease with increasing temperature, indicating a reduction of the magnetocrystalline anisotropy energy. The magnetization steps during the field-induced transitions also decrease with increasing temperature from  $\sim 0.8\mu_B$  at 10 K to  $\sim 0.3\mu_B$  at 40 K to zero at 70 K, reasonably closely following the decrease of tilting angles of magnetic moments with the  $a$  axis. The field-induced transition along the  $b$  axis also disappears at  $T_{\text{SR}}=70$  K. The magnetization at 70 kOe and 70 K is

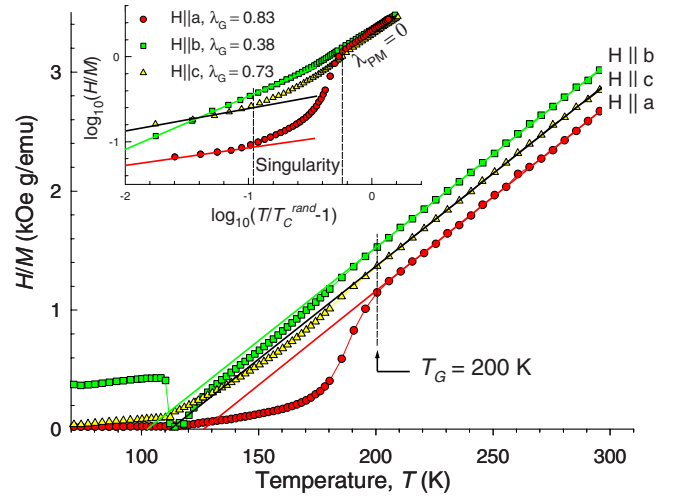


FIG. 6. (Color online) The inverse dc magnetic susceptibility ( $H/M$ ) of single-crystal  $\text{Tb}_5\text{Si}_{2.2}\text{Ge}_{1.8}$  measured in a 10 Oe magnetic field applied along the  $a$ ,  $b$ , and  $c$  axes during FC heating. The inset illustrates  $\log_{10}(H/M)$  vs  $\log_{10}(T/T_C^{\text{rand}}-1)$  for the main panel data. Solid lines represent Curie-Weiss fits in the main panel, and linear fits of  $\log_{10}(H/M)$  vs  $\log_{10}(T/T_C^{\text{rand}}-1)$  to establish  $\lambda$  in  $\chi^{-1} \propto (T-T_C^{\text{rand}})^{1-\lambda}$  in the inset.

$4.3\mu_B$ , which is close to that at 70 kOe and 40 K ( $4.9\mu_B$ ). Therefore, the absence of a sharp field-induced transition along the  $b$  axis at and above 70 K indicates that the Tb moments are coherently rotated from the  $ac$  plane to the  $b$  axis upon the increasing of the external magnetic field.

The magnetization isotherms with the applied field along the  $c$ -axis direction show a departure from the ferromagnetic behavior with increasing temperature, which is consistent with the tilting of the magnetic moments away from this direction when temperature increases from 1.8 to 70 K. No field-induced magnetic phase transition with  $\mathbf{H}\parallel\mathbf{c}$  is observed in Fig. 5. Therefore, between 1.8 and 70 K, the field-induced magnetic phase transitions occur with  $\mathbf{H}\parallel\mathbf{a}$  and  $\mathbf{H}\parallel\mathbf{b}$ , but not with  $\mathbf{H}\parallel\mathbf{c}$  when the magnetic field is less than 70 kOe. On the contrary, when temperatures are in the vicinity of or above the  $T_C$  of  $\text{Tb}_5\text{Si}_{2.2}\text{Ge}_{1.8}$ , field-induced magnetic phase transitions occur when the external field is along the  $a$  and  $c$  axes directions but not the  $b$  axis (see Figs. 1 and 2 in Ref. 13). This difference suggests a strong thermal variation of the magnetic anisotropy energy.

Figure 6 illustrates the temperature dependencies of the inverse dc magnetic susceptibilities ( $H/M$ ) of  $\text{Tb}_5\text{Si}_{2.2}\text{Ge}_{1.8}$  measured during FC heating from 1.8 to 300 K with a 10 Oe magnetic field applied along the  $a$ ,  $b$ , and  $c$  axes. The Griffiths phaselike behavior is evident by a characteristic negative deviation<sup>19</sup> from the Curie-Weiss behavior and less-than-unity magnetic-susceptibility exponents<sup>20</sup> between  $T_C$  ( $118 \pm 2$  K) and  $T_G$ . The latter is the critical Griffiths temperature of  $200 \pm 2$  K as marked in Fig. 6, taken as the temperature where the  $H/M$  curves start deviating from the Curie-Weiss behavior. The inset of Fig. 6 shows the logarithmic representation of the main panel data ( $H/M$  vs  $T$ ) and their fitting to the relation  $\chi^{-1} \propto (T-T_C^{\text{rand}})^{1-\lambda}$ , where  $T_C^{\text{rand}}$  is an adjustable parameter, and  $\lambda$  is the magnetic-susceptibility exponent parameter. In the conventional paramagnetic phase

above  $T_G$ ,  $\lambda_{PM}$  is zero and isotropic. In the Griffiths phase regime between  $T_C^{rand}$  and  $T_G$ , both the negative deviations and  $\lambda_G$  are anisotropic. The most pronounced negative deviation and the largest  $\lambda_G$  are found when the magnetic field is parallel to the  $a$  axis, which is the magnetic easy axis at temperatures below  $T_C$ . This observation is in line with the report that in single crystal  $Gd_5Ge_4$  the magnetic susceptibility along its easy magnetization direction always exhibits a greater deviation from Curie-Weiss behavior when compared to the other two major crystallographic directions below its  $T_G$ .<sup>16</sup> The observed anisotropy is reasonable considering that the Griffiths-like phase originates from a system of ferromagnetic clusters in the paramagnetic phases of both single-crystal  $Gd_5Ge_4$  and polycrystalline  $Tb_5Si_2Ge_2$ .<sup>15,16</sup>

It is interesting to note that the differences in Weiss temperatures are consistent with the anisotropy of the layered crystal structure (see Fig. 1) of the compound and are consistent with the current understanding of the nature of magnetic exchange interactions in the family of  $R_5T_4$  compounds, where  $T$  is Si or Ge. It is known that the  $-R-T-T-R$ -network plays a significant role in defining magnetic interactions.<sup>21,22</sup> Within each slab, the network of strongly interacting-Tb1-T1-T2-Tb1-atoms is two dimensional and it remains intact in both the paramagnetic and magnetically ordered states. The three dimensionality of the network is restored only in the magnetically ordered state when the monoclinic phase transforms into the orthorhombic  $Tb_5Si_{2.2}Ge_{1.8}$  in which the -Tb1-T3-T3-Tb1- network also exists (it is absent on the monoclinic phase where T3-T3 bonds are too long). Hence, strong pseudo-two-dimensional interactions in the planes of the slabs ( $ac$  plane) are reflected in the higher Weiss temperatures for  $\mathbf{H}\parallel\mathbf{a}$  and  $\mathbf{H}\parallel\mathbf{c}$ .

The anisotropy of the ferromagnetic clusters in the Griffiths phaselike state of  $Tb_5Si_{2.2}Ge_{1.8}$  is also evident from the thermal history dependence of the dc magnetization measured in a 10 Oe applied magnetic field when  $T_C < T < 150$  K, Fig. 7. Here, the magnitude of magnetization is substantially greater when  $T_C$  is approached upon cooling than upon heating. This difference is greater the closer the system is to  $T_C$ . The resulting inverse thermal hysteresis, which is in contrast to a conventional thermal hysteresis where the magnetization measured at the same temperature upon heating is greater than that upon cooling (see Fig. 3), occurs because the magnetic and crystallographic phase transitions in the  $Tb_5Si_{2.2}Ge_{1.8}$  compound are decoupled by less than 5 K in zero and weak applied magnetic fields. Thus, the magnetic ordering on cooling starts with the ferromagnetic ordering of the monoclinic phase.<sup>10</sup> This second order, purely magnetic phase transition, is preceded by growth of both the size and number of the monoclinic ferromagnetic clusters, which is responsible for the rapid increase of the magnetization when the temperature approaches 117 K from  $T > T_C$  (Fig. 7). The drastic decrease of the magnetization from 117 to 115 K when  $\mathbf{H}\parallel\mathbf{a}$  and  $\mathbf{H}\parallel\mathbf{b}$  may be understood if one assumes that the crystallographic phase transition from the monoclinic to orthorhombic phase occurs over this temperature range. It has been established both theoretically<sup>21</sup> and experimentally<sup>23</sup> that in the closely related  $R_5T_4$  compounds with  $R=Gd$ , the Curie temperature of the orthorhombic  $Gd_5Si_4$ -type polymorph is much higher than that of the

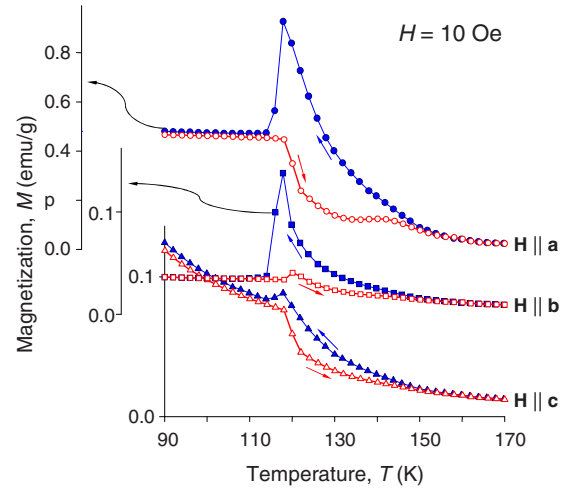


FIG. 7. (Color online) Temperature dependencies of the magnetization of single-crystal  $Tb_5Si_{2.2}Ge_{1.8}$  measured in a 10 Oe magnetic field applied parallel to the  $a$ ,  $b$ , and  $c$  axes upon FC heating (open symbols) and FH cooling (solid symbols). Note that the temperature scale is the same for the three orientations.

monoclinic  $Gd_5Si_2Ge_2$ -type phase. By analogy, and also considering preliminary theoretical modeling results,<sup>24</sup> the orthorhombic  $Tb_5Si_{2.2}Ge_{1.8}$  has a higher  $T_C$  when compared to the monoclinic  $Tb_5Si_{2.2}Ge_{1.8}$ . Thus, on cooling to 115 K much of the monoclinic ferromagnetic  $Tb_5Si_{2.2}Ge_{1.8}$  single crystal transforms to the orthorhombic ferromagnetic structure, and  $T_C$  of the latter is considerably greater than 115 K. Given that anisotropy constants generally increase when temperature is below  $T_C$ , and considering a strong single-ion anisotropy of the  $Tb^{3+}$  ion, the anisotropy energy of the orthorhombic ferromagnetic  $Tb_5Si_{2.2}Ge_{1.8}$  is expected to be much greater than that of the monoclinic ferromagnetic  $Tb_5Si_{2.2}Ge_{1.8}$  at 115 K. Obviously, the orthorhombic magnetic domains form concurrently with the crystallographic phase transformation. Yet, a 10 Oe field is not large enough to move the domain walls of the orthorhombic ferromagnetic  $Tb_5Si_{2.2}Ge_{1.8}$  at 115 K. This leads to an abrupt decrease of the magnetization values upon cooling through the crystallographic phase-transition temperature. On heating, the structural transition is shifted by 4 to 5 K toward higher temperature,<sup>13</sup> but the  $T_C$  of the monoclinic phase remains the same, and overall, the transition is between the orthorhombic ferromagnetic and the monoclinic paramagnetic polymorphs of  $Tb_5Si_{2.2}Ge_{1.8}$ . As a result, the magnetization values measured on heating are lower than those during cooling.

This model of the anomalous thermal hysteresis in  $Tb_5Si_{2.2}Ge_{1.8}$  when  $T_C < T < 150$  K is supported by the following observations. First, the inverse hysteresis disappears along the  $a$  and  $c$  axes when the field is increased to 1000 Oe, as shown in Fig. 8, indicating that coercive fields along these two directions are lower than 1000 Oe. Second, the thermal history dependencies of the magnetization in a 100 Oe magnetic field (see Fig. 9) applied along the  $a$  and  $c$  axes show a crossover behavior between the 10 and 1000 Oe field data. Finally, the thermal irreversibility near  $T_C$  remains unconventional and abnormal along the  $b$  axis even in fields as

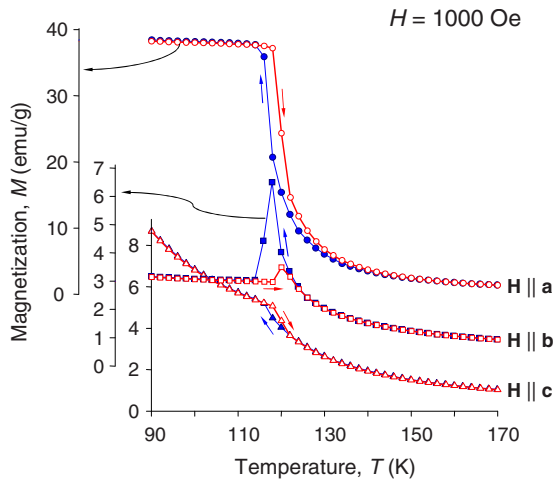


FIG. 8. (Color online) Temperature dependencies of the magnetization of single-crystal  $\text{Tb}_5\text{Si}_{2.2}\text{Ge}_{1.8}$  measured in a 1000 Oe magnetic field applied parallel to the  $a$ ,  $b$ , and  $c$  axes upon FC heating (open symbols) and FH cooling (solid symbols). Note that the temperature scale is the same for the three orientations.

high as 10 kOe (see Figs. 2 and 7–9). In other words, while the thermal irreversibility anomalies may be suppressed by the external magnetic field, it is most difficult to do so with the field along the  $b$  axis. This is consistent with the  $b$  axis being the magnetically hard axis, and the  $a$  axis (and the  $c$  axis) being the easy axes of the orthorhombic  $\text{Tb}_5\text{Si}_{2.2}\text{Ge}_{1.8}$  compound as seen in Figs. 4 and 5. It is well known that when a magnetic field is applied parallel to the easy axis in a demagnetized system, domain-wall displacements dominate the magnetization process, which is on the other hand dominated by spin rotations when the applied field is parallel to the hard axis of a system with a strong intrinsic anisotropy. Consequently, domain walls are easier to move when the magnetic field is applied along the  $a$  and  $c$  axes than the  $b$  axis of the  $\text{Tb}_5\text{Si}_{2.2}\text{Ge}_{1.8}$  single crystal, leading to a much

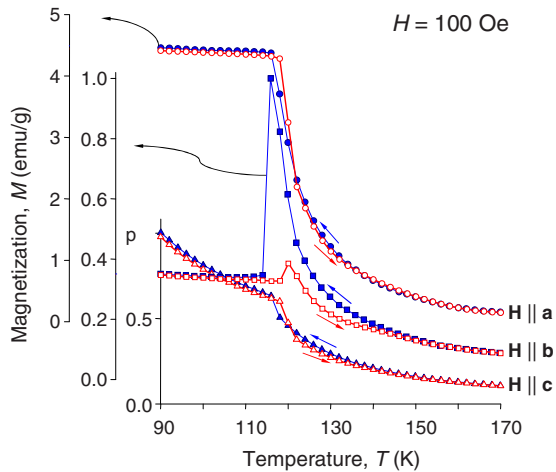


FIG. 9. (Color online) Temperature dependencies of the magnetization of single-crystal  $\text{Tb}_5\text{Si}_{2.2}\text{Ge}_{1.8}$  measured in a 100 Oe magnetic field applied parallel to the  $a$ ,  $b$ , and  $c$  axes upon FC heating (open symbols) and FH cooling (solid symbols). Note that the temperature scale is the same for the three orientations.

more persistent hysteresis anomaly along the  $b$  axis.

The larger magnitude of magnetization upon FH cooling when compared to FC heating in small magnetic fields (but not the sharp drop during cooling as in  $\text{Tb}_5\text{Si}_{2.2}\text{Ge}_{1.8}$ ) has also been observed in a  $\text{Gd}_5\text{Ge}_4$  single crystal. It was ascribed to short-range ferromagnetic correlations in both the paramagnetic and antiferromagnetic phases of the compound.<sup>16</sup> These short-range ferromagnetic correlations originate from a competition between the interslab and intraslab magnetic exchange interactions. In the  $\text{Tb}_5\text{Si}_{2.2}\text{Ge}_{1.8}$  compound, the anomalous hysteresis away from  $T_C$  is of a similar origin as the one in the  $\text{Gd}_5\text{Ge}_4$  compound, but it is

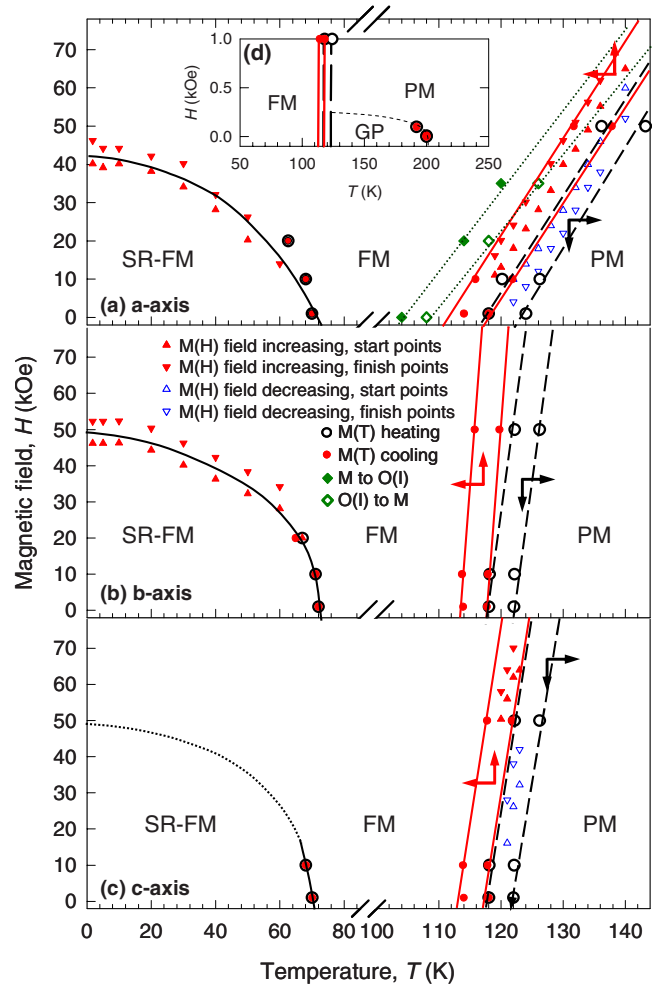


FIG. 10. (Color online) The temperature-magnetic-field phase diagrams with field applied along the  $a$ ,  $b$ , and  $c$  axes of  $\text{Tb}_5\text{Si}_{2.2}\text{Ge}_{1.8}$ . The solid and open circles represent critical temperatures from isofield  $M(T)$  data upon ZFC heating and FH cooling, respectively; the solid and open triangles represent critical magnetic fields derived from the isothermal  $M(H)$  data upon field increasing and decreasing, respectively. The solid and open diamonds in (a) represent the midpoints of the crystallographic phase transformations derived from the *in situ* x-ray powder-diffraction data of Ref. 13. Panel (d) illustrates the Griffiths phase boundary derived from the low-field  $M(T)$  data with  $\mathbf{H} \parallel \mathbf{a}$ . The lines are guides to the eye. Arrows placed between the boundaries indicate phase separated regions for the corresponding directions of the temperature and magnetic field changes.



the decoupling of the magnetic and crystallographic phase transitions that defines the anomalous behavior of the magnetization in the immediate vicinity of  $T_C$ .

Conventional hysteresis occurring at  $T_C$  when the 1000 Oe magnetic field is applied along the  $a$  and  $c$  axes has two factors in its origin. First, with increasing external field, the contribution from ferromagnetic clusters (Griffiths phase) becomes less visible (is quenched) due to an increased contribution from the paramagnetic matrix. Second, at  $T < T_C$ , the net magnetization increases because the external field exceeding the coercive field increases the volume of the domains with spins oriented in the direction favored by the external field. At  $T_C$ , the magnetization from ferromagnetic monoclinic  $\text{Tb}_5\text{Si}_{2.2}\text{Ge}_{1.8}$  is no longer greater than that from the oriented magnetic domains of the orthorhombic phase of the compound, therefore, normal hysteresis corresponding to a first-order magnetic phase transition sets in. Obviously, this critical field should be markedly different along different crystallographic directions due to strong magnetocrystalline anisotropy below  $T_C$ . The persistence of the inverse hysteresis at 10 kOe applied along the magnetic hard  $b$  axis is the manifestation of this mechanism.

Based upon the magnetization data from the present and previous<sup>13</sup> studies, the magnetic phase diagrams of  $\text{Tb}_5\text{Si}_{2.2}\text{Ge}_{1.8}$  with the magnetic field applied along the three major crystallographic directions are constructed and displayed in Fig. 10. It is worth mentioning that the  $M(H)$  and  $M(T)$  data are in excellent agreement with one another. The magnetically ordered phases are denoted as FM for the canted ferromagnetic structure observed in a zero magnetic field between  $T_{\text{SR}}$  and  $T_C$ , and SR-FM for a different canted ferromagnetic structure, which is observed in a zero field below  $T_{\text{SR}}$ . The phase boundaries separating SR-FM and FM states with  $\mathbf{H}\parallel\mathbf{a}$  and  $\mathbf{H}\parallel\mathbf{b}$  closely follow one another, but they do not coincide. A similar phase boundary when  $\mathbf{H}\parallel\mathbf{c}$  cannot be traced using  $M(H)$  behavior because no obvious field-induced phase transition is observed here. These phase diagrams show a strong anisotropic behavior of the magnetic order-disorder transitions. Phase boundaries between the paramagnetic (PM) and magnetically ordered states for the three directions are considerably different from each other. For instance, magnetic field applied along the  $a$  axis has a strong effect on  $T_C$  ( $dT_C/dH$  approaches 0.4 K/kOe). On the other hand, when the field is applied along the  $b$  and  $c$  axes,  $dT_C/dH$  is lower by a factor of 4 to 5.

#### IV. CONCLUSIONS

The ordering temperatures and thermal hystereses of the magnetic order-disorder transition in  $\text{Tb}_5\text{Si}_{2.2}\text{Ge}_{1.8}$  are highly anisotropic when an applied magnetic field reaches and exceeds 10 kOe. The temperature-induced spin reorientation transition occurring at  $\sim 70$  K in a zero magnetic field is clearly observed from  $M(T)$  data collected with fields below 10 kOe applied along all three principal crystallographic axes. It becomes less visible and shifts to lower temperatures with  $\mathbf{H}\parallel\mathbf{b}$ , or becomes undetectable with  $\mathbf{H}\parallel\mathbf{a}$  and  $\mathbf{H}\parallel\mathbf{c}$  in a 50 kOe external field. Field-induced magnetic phase transitions have been observed between 1.8 and 70 K with  $\mathbf{H}\parallel\mathbf{a}$  and  $\mathbf{H}\parallel\mathbf{b}$ , but not  $\mathbf{H}\parallel\mathbf{c}$ .

The anisotropic Griffiths phaselike behavior has been observed above  $T_C$  in the temperature dependencies of magnetization measured in 10, 100, and 1000 kOe magnetic fields. Below  $\sim 150$  K and above  $T_C$ , the magnetic-susceptibility exponent exhibits the largest negative deviation from unity when  $\mathbf{H}\parallel\mathbf{a}$ . The anisotropy of the Griffiths-like phase behavior originates from anisotropic ferromagnetic short-range order when  $T_C < T < \sim 150$  K. The anomalous separation of the heating and cooling magnetization curves observed in low applied magnetic fields in this temperature range is most persistent with the magnetic field applied along the  $b$  axis. Anomalies in thermal history dependencies of magnetization above  $T_C$  confirm the decoupling of the magnetic and crystallographic phase transformations. A model involving magnetic domain effects in the long-range ordered state of the  $\text{Tb}_5\text{Si}_{2.2}\text{Ge}_{1.8}$  compound has been proposed to explain anomalous thermal history in the vicinity of  $T_C$ . Strong magnetocrystalline anisotropy of the compound is reflected in the anisotropic field-temperature phase diagrams constructed for the three independent crystallographic directions.

#### ACKNOWLEDGMENTS

Different aspects of this work were supported by the U.S. Department of Energy, Office of Basic Energy Sciences, Materials Sciences Division and NASA under NNL-05-AA198. The Ames Laboratory is operated for the U.S. DOE by Iowa State University under Contract No. DE-AC02-07CH11358.

\*Corresponding author; vitkp@ameslab.gov

<sup>1</sup>V. K. Pecharsky and K. A. Gschneidner, Jr., Phys. Rev. Lett. **78**, 4494 (1997).

<sup>2</sup>L. Morellon, P. A. Algarabel, M. R. Ibarra, J. Blasco, B. Garcia-Landa, Z. Arnold, and F. Albertini, Phys. Rev. B **58**, R14721 (1998).

<sup>3</sup>L. Morellon, J. Stankiewicz, B. Garcia-Landa, P. A. Algarabel, and M. R. Ibarra, Appl. Phys. Lett. **73**, 3462 (1998).

<sup>4</sup>E. M. Levin, V. K. Pecharsky, and K. A. Gschneidner, Jr., Phys. Rev. B **63**, 174110 (2001).

<sup>5</sup>V. K. Pecharsky and K. A. Gschneidner, Jr., Adv. Mater. (Wein-

heim, Ger.) **13**, 683 (2001).

<sup>6</sup>L. Morellon, C. Magen, P. A. Algarabel, M. R. Ibarra, and C. Ritter, Appl. Phys. Lett. **79**, 1318 (2001).

<sup>7</sup>O. Tegus, W. Dagula, E. Brück, L. Zhang, F. R. Boer, and K. H. J. Buschow, J. Appl. Phys. **91**, 8534 (2002).

<sup>8</sup>H. Huang, A. O. Pecharsky, V. K. Pecharsky, and K. A. Gschneidner, Jr., Adv. Cryog. Eng. **47A**, 11 (2002).

<sup>9</sup>C. Ritter, L. Morellon, P. A. Algarabel, C. Magen, and M. R. Ibarra, Phys. Rev. B **65**, 094405 (2002).

<sup>10</sup>L. Morellon, C. Ritter, C. Magen, P. A. Algarabel, and M. R. Ibarra, Phys. Rev. B **68**, 024417 (2003).



- <sup>11</sup>V. O. Garlea, J. L. Zarestky, C. Y. Jones, L.-L. Lin, D. L. Schlagel, T. A. Lograsso, A. O. Tsokol, V. K. Pecharsky, K. A. Gschneidner, Jr., and C. Stassis, *Phys. Rev. B* **72**, 104431 (2005).
- <sup>12</sup>L. Morellon, Z. Arnold, C. Magen, C. Ritter, O. Prokhnenko, Y. Skorokhod, P. A. Algarabel, M. R. Ibarra, and J. Kamarad, *Phys. Rev. Lett.* **93**, 137201 (2004).
- <sup>13</sup>M. Zou, Ya. Mudryk, V. K. Pecharsky, K. A. Gschneidner, Jr., D. L. Schlagel, and T. A. Lograsso, *Phys. Rev. B* **75**, 024418 (2007).
- <sup>14</sup>Z. W. Du, A. S. Liu, B. L. Shao, Z. Y. Zhang, X. S. Zhang, and Z. M. Sun, *Mater. Charact.* (to be published).
- <sup>15</sup>C. Magen, P. A. Algarabel, L. Morellon, J. P. Araújo, C. Ritter, M. R. Ibarra, A. M. Pereira, and J. B. Sousa, *Phys. Rev. Lett.* **96**, 167201 (2006).
- <sup>16</sup>Z. W. Ouyang, V. K. Pecharsky, K. A. Gschneidner, Jr., D. L. Schlagel, and T. A. Lograsso, *Phys. Rev. B* **74**, 094404 (2006).
- <sup>17</sup>D. L. Schlagel, T. A. Lograsso, A. O. Pecharsky, and J. A. Sampaio, in *Light Metals 2005*, edited by H. Kvande (The Minerals, Metals and Materials Society, Warrendale, PA, 2005), p. 1177.
- <sup>18</sup>Materials Preparation Center, Ames Laboratory of U.S. DOE, Ames, IA ([www.mpc.ameslab.gov](http://www.mpc.ameslab.gov)).
- <sup>19</sup>M. B. Salamon, P. Lin, and S. H. Chun, *Phys. Rev. Lett.* **88**, 197203 (2002).
- <sup>20</sup>A. H. Castro Neto, G. Castilla, and B. A. Jones, *Phys. Rev. Lett.* **81**, 3531 (1998).
- <sup>21</sup>D. Paudyal, V. K. Pecharsky, K. A. Gschneidner, Jr., and B. N. Harmon, *Phys. Rev. B* **73**, 144406 (2006).
- <sup>22</sup>D. Haskel, Y. B. Lee, B. N. Harmon, Z. Islam, J. C. Lang, G. Srajer, Ya. Mudryk, K. A. Gschneidner, Jr., and V. K. Pecharsky, *Phys. Rev. Lett.* **98**, 247205 (2007).
- <sup>23</sup>V. K. Pecharsky, G. D. Samolyuk, V. P. Antropov, A. O. Pecharsky, and K. A. Gschneidner, Jr., *J. Solid State Chem.* **171**, 57 (2003).
- <sup>24</sup>D. Paudyal, V. K. Pecharsky, and K. A. Gschneidner, Jr. (unpublished).